

# Optimal cutting conditions of abrasive waterjet cutting for Ti-6Al-2Sn-4Zr-2Mo alpha-beta alloy using the Aquila algorithm method

Ugochukwu Sixtus Nwankiti<sup>1</sup>, Adeyinka Oluwo<sup>1</sup>, Bayo Yemisi Ogunmola<sup>1</sup>, John Rajan<sup>2</sup>, Swaminathan Jose<sup>3</sup>, Sunday Ayoola Oke<sup>1\*</sup>, Boluvar Lathashankar<sup>4</sup>, and Ayomide Sunday Ibitoye<sup>1</sup>

<sup>1</sup> Department of Mechanical Engineering, University of Lagos, Lagos 101245, Nigeria

<sup>2</sup> Department of Manufacturing Engineering, Vellore Institute of Technology, Chennai 600127, India

<sup>3</sup> School of Mechanical Engineering, Vellore Institute of Technology, Vellore 632014, India

<sup>4</sup> Department of Industrial Engineering and Management, Siddaganga Institute of Technology, Karnataka 572103, India

## ABSTRACT

**\*Corresponding author:**

Sunday Ayoola Oke  
sa\_oke@yahoo.com

**Received:** 19 April 2024

**Revised:** 30 July 2024

**Accepted:** 24 August 2024

**Published:** 2 October 2025

### Citation:

Nwankiti, U. S., Oluwo, A., Ogunmola, B. Y., Rajan, J., Jose, S., Oke, S. A., Lathashankar, B., & Ibitoye, A. S. (2025). Optimal cutting conditions of abrasive waterjet cutting for Ti-6Al-2Sn-4Zr-2Mo alpha-beta alloy using the Aquila algorithm method. *Science, Engineering and Health Studies*, 19, 25040001.

This article introduces a novel method, namely the Aquila algorithm for optimizing the abrasive waterjet cutting process for machining Ti-6Al-2Sn-4Zr-2Mo alpha-beta alloy. The main parameters of the process are the waterjet pressure (WJP), traverse speed (TS) and the stand-off distance (SOD), while material removal rate (MRR) and surface roughness (Ra) are its responses. The Aquila algorithm optimizes the process parameters, thereby declaring the optimal thresholds for improved efficiency. Unlike previous studies, this work accounts for the optimization of the abrasive waterjet cutting parameters, providing direction on how much of each parameter to utilize for optimal performance of the system. Experimental data from the published literature was used to validate the proposed model. After performing the analysis, the optimal parameters at the convergence of the results after 300 iterations were WJP, TS, SOD, and MRR of 260 bar, 40 mm/min, 3 mm, and 164.74 mm<sup>3</sup>/min, respectively. This is when the response considered is the material removal rate. Considering the surface roughness as the output, the optimal solutions for WJP, TS, SOD, and SR were 256.27 bar, 24.54 mm<sup>3</sup>/min, 1.00 mm, and 2.54 mm<sup>3</sup>/min, respectively. The outcomes will assist process engineers in using optimal results for efficient decision-making in the abrasive waterjet machining process for the Ti-6Al-2Sn-4Zr-2Mo alpha-beta alloy.

**Keywords:** optimization; efficiency; waterjet; machining; parameters

## 1. INTRODUCTION

The machining industry has recently suffered some setbacks due to the rising cost of labor, skill set deficiency, and the COVID-19 pandemic, which have restricted business operations globally (Mezgebe et al., 2023; Halteh et al., 2024; Nakandala, 2024). Therefore, great importance must be paid to performance monitoring and accountability at

machining work centers (Pancaldi et al., 2023; Hussain et al., 2024; Xu et al., 2024). At present researchers attach much concern to optimization schemes in the machining domain (Fan et al., 2024; Zhang et al., 2024). However, despite the various machining types and technology, abrasive waterjet cutting has seemingly become a key machining type of interest to investigators (Thakur et al., 2021; Tripathi et al., 2021). Although first introduced by

Leslie Turel and Elmo Smith in about 1935, to allow cutting through tough materials, interest in abrasive waterjet cutting technology was sustained when it was noticeable that the process could cut complicated contours and a broad range of materials (Sadasivam & Arola, 2012). Consequent upon the changing needs of the aerospace industry, some researchers, including Perumal et al. (2020), Tripathi et al. (2021), Kant and Dhami (2021) investigated the optimization and parametric characteristics of aerospace materials. Among these researchers, Perumal et al. (2020) stand out in their analysis of the Ti-6Al-2Sn-4Zr-2Mo alpha-beta alloy, which incorporates aluminium or vanadium as alloying elements for corrosion resistance and stability at elevated temperatures. The article dwelt on parametric optimization for the unique aerospace structural metal named Ti-6Al-2Sn-4Zr-2Mo alpha-beta alloy.

From the above discussion, it has been established that optimization in abrasive waterjet cutting is important (Naresh Babu & Muthukrishnan, 2015). The Ti-6Al-2Sn-4Zr-2Mo alpha-beta alloy is key to the material development structural design and maintenance of the aerospace industry (Perumal et al., 2020). On the strength of the scenario described above, the optimization of process parameters in the abrasive waterjet cutting of Ti-6Al-2Sn-4Zr-2Mo alpha-beta alloy was pursued in this paper. The experimental data of Perumal et al. (2020) was analyzed for the deployment of the new algorithm called Aquila to demonstrate the feasibility of its application to the problem for optimization purposes. The parameters used were the abrasive waterjet pressure, traverse speed and stand-off distance. To start the cutting using the waterjet, which has abrasive metals dissolved in it, it was conceptualized that there should be regulation to some pressure quantities that must be known. Concurrently, the speed at which the waterjet discharges from the pipe should be set to a reasonable level that is not too high or too low to aid fast completion of the job. Also, as the process involves risks that should be eliminated, it is known that effective cutting of the alloy may not be achieved without maintaining some distances from the cutting surface of the alloy (i.e., the distance is called the stand-off distance). At present in literature, only the best parameters at which resources may be channeled are known. At what particular pressure, traverse speed and stand-off distance the cutting operation should be conducted at are unknown. At the best, the machining manager uses experience and intuition to decide on these parameters. The implication of this is that, inadequate values are used for decision making and serious material losses, machine hours and manhours may be incurred. However, the case may change if appropriate parametric values at optimal conditions are used. Thus, there is a research gap in transiting from the use of sub-optimal values to optimal values. Therefore, a solution approach, using mathematical methods is required to fill this research gap.

Moreover, the present research explores the optimization of cutting conditions in abrasive waterjet machining, addressing the research gap of sparse quantitative optimisation measures, unexplored in a previous related article by Nwankiti and Oke (2022). In Nwankiti and Oke (2022), the authors employed the EDAS method and the desirability function analysis, which allows a deep understanding of how the best abrasive waterjet cutting

conditions can be selected. They further analyzed how single outcomes of the study, each for the material removal rate and surface roughness, could be integrated into a holistic result. However, building on the results of Nwankiti and Oke (2022), and the unique elements of the Aquila algorithm in exploration and exploitation activities, the present study develops a scheme in the Aquila algorithm to test the impact of the exploration and exploitation activities on the attainment of optimal results instead of the sub-optimal outcomes, which the EDAS and DFA methods, intuition and the experience of the process engineer offer. The results of the present study thus offer the first quantitative evidence of optimizing parameters while dealing with a unique alloy named the Ti-6Al-2Sn-4Zr-2Mo alpha-beta alloy. This sets a standard against which current achievements at the factory floor may be compared.

Furthermore, this study uses the Aquila algorithm as a preferred optimization tool, to solve the abrasive waterjet optimization problem while machining the Ti-6Al-2Sn-4Zr-2Mo alpha-beta alloy because of its distinct attributes. First, the Aquila algorithm has multiple exploration methods for effective optimization decisions. The Aquila may choose the appropriate method according to the characteristics of the prey being hunted: size, shape, strength, and ability/inability among others, to move from one location to another. Concurrently, the Aquila algorithm possesses strong optimization potential, a fast convergence speed and a mature algorithm.

### 1.1 Background

In this article, the literature review is presented to offer background information on the subject considered and showcase the importance of the present study by bridging the identified gap in the literature. A literature review is conducted on the parameters used in abrasive waterjet machining and the mathematical models employed, particularly when utilizing Ti-6Al-2Sn-4Zr-2Mo alpha-beta alloy. To understand these parameters, a comprehensive investigation of the various abrasive waterjet process parameters was conducted and the details are shown as follows: Ishfaq et al. (2019) investigated the capacity of abrasive waterjet cutting for the cutting of steel cladding with stainless steel by enhancing the rate of material removal and ensuring little kerf taper as the focal point. The results showed that the mass flow of the abrasive and the feed rate were the most influential factors for both conditions (enhanced rate of material removal and minimized kerf taper) to be met. Karakurt et al. (2012) explored the use of abrasive waterjet for cutting granite, focusing on the effect of the textural qualities of the granite and the operation conditions on the depth of cut and cut surface finish of the granite. They discovered that the cutting speed across the granite greatly affected the depth of the cut. Also, the grain size and its placement with its surroundings affect the cut depth and the cut surface finish. Wang and Zhong (2009) conducted an experiment on the cut depth of alumina ceramics with AWJ (abrasive waterjet) by proposing a technique of cutting, which makes use of multipass operations alongside controlled nozzle oscillation. They discovered that the cut depth can be raised by 50.8% average within a duration using multipass cutting alongside nozzle oscillations unlike when using single-pass cutting alone. Srinivas and Ramesh Babu (2012) determined the penetration capability of

AWJs on various structures of aluminium-silicon carbide particulate metal matrix composites (Al-Sc MMCS) that were created by stir casting. They found that the mass flow rate of the abrasive used and the cutting traverse speed matched the optimum level for Al-Sc MMCs using AWJs. Zhong and Han (2002) explored the turning of 25 mm diameter glass rods using abrasive waterjets with a focus on the effect of the operating factors on the surface finish of the glass rods. They found that surface finish was highly dependent on the turning speed compared to the jet traverse speed. High jet traverse speeds generally lead to poor surface finish while low traverse speed and fast turning speeds give a relatively better finish.

Wang et al. (2003) tested how to improve the cutting-ability in AWJ operations using multipass cutting and forward impact angle methods; both one at a time and simultaneously. They discovered that when making use of the multipass cutting method alongside an 80° forward angle it gives the best results for machining alumina ceramics. Tripathi et al. (2021) studied the effects of abrasive waterjet machining conditions on glass fiber-reinforced polymer (GFRP) using the flow rate of abrasives and the cutting speed as the two conditions of interest. After using Rao algorithms, the optimum values for the speed of cutting and abrasive flow rate were obtained as 100cm per minute and 300 gm per minute, respectively. Kant and Dhami (2021) studied the effects of jet traverse speed, mass flow rate of the abrasive stand-off distance and pressure on the hardness, operating time and surface finish, and how to optimize these parameters.

Li et al. (2016) used AWJs in single-pass-radial-mode for machining PEEK (polyetheretherketone) strengthened with carbon-fiber to recognize the consequence of the water pressure, nozzle tilt angle, speed of rotating surface, feed speed and mass flow rate of the abrasive used on the surface quality, the rate of cutting/MRR (material removal rate) and the achieved depth of cut. They recognized that when large values of water pressure and rotating speed are used with the standard nozzle tilt angle and satisfactory feed rate and mass flow rate of abrasive, the process yields a high material removal rate with minimal effects on the surface finish quality. Kalirasu et al. (2018) studied the execution of cutting operations using abrasive waterjets on CS/UPR (coconut sheath/unsaturated polyester) combined materials that have been treated using NaOH (sodium hydroxide) and C<sub>2</sub>H<sub>3</sub>Cl<sub>3</sub>Si (trichlorovinylsilane), respectively. The materials treated with saline had a 12% and 22% decrease in kerf taper angle and surface quality (roughness), respectively, in contrast to the crude materials. They also found several failure conditions (pullouts, breakage, voids matrix failure and debonding) in the materials when examined with the electron microscope.

Boud et al. (2014) studied the usage of abrasives that are dissoluble in water as an alternative to insoluble abrasives, negating their adverse effects especially the lodging of said abrasive on the material's surface profile. Testing showed that the soluble abrasives yielded better results for the rate of material removal compared to ordinary waterjet cutting operations. Sadasivam and Arola (2012) studied the dependency of the quantity and depth of residual stress on the circumstance of the boundary considering pre-stress values from a minimum of 0 to a maximum of 75%. It was established that the depth of the altered material region underneath the work surface

depends on the boundary conditions while the region experiencing left-over stress is barely affected.

Ay et al. (2010) researched the behavior of abrasive waterjet cutting processes done on Inconel 718 nickel-based superalloy when operated with different cutting speeds (traverse speed) ranging from 80 mm/min to 330 mm/min. The test results showed that the kerf taper ratio and unevenness of the work surface directly vary with the cut-through speed while the cutting kerf varies inversely with the cut-through speed (traverse speed). Yuvaraj and Kumar (2017) examined the abrasive waterjet cutting of aluminium alloy (AA5083-H32) and the effects of jet inclination angle on to work surface and the abrasive structural sizes under multiple water pressures on the characteristics of the finished product. They found that slant placement of the jet greatly affects the outcome of the operation and the structural size of the abrasive has varying effects as it improves some while deteriorating others simultaneously. Chakraborty and Mitra (2018) used GWO (Grey Wolf Optimizer) to determine the best control values for abrasive waterjet cutting operations. The obtained outcome gave a noticeably better result than other analysis tools used before GWO.

Zhang and Li (2010) used abrasive waterjet for machining delicate materials that are either composites or ceramic. They are focused on the effects of using AWJs on brittle materials and figuring out an optimal approach to boring holes without causing irreparable damages that will affect the life of the materials. Naresh Babu and Muthukrishnan (2015) used Taguchi orthogonal array and grey relational analysis for the enhancement of AWJ cutting processes based on the operating conditions such as the material feed rate, jet pressure/intensity, stand-off distance, mass flow rate of the abrasive and the diameter of the nozzle used on the quality of the finished product and its characteristics. They discovered from the analysis performed, that there was a lower roughness and kerf size values for the best operating conditions. Thakur et al. (2021) studied the conditions for operating the AWJs when nanoclay is used as a subordinate strengthener for carbon-epoxy materials. The water jet pressure was tested for values of 96 and 304MPa, the cut-through speed was tested for 50 through 150 mm per minute with an increment of 50 mm per minute in between. The amount of nanoclay used was increased from none to 1.25% and then to 2.50% weight of the whole material. It was noticed that CFRP materials infused with nanoclay had lesser values for material removal rate and roughness of surface than the ones without nanoclay.

## 2. MATERIALS AND METHODS

### 2.1 Justification for the optimization method used in the study

In the optimization context, there exist two broad categories of optimization problems, namely the conventional and non-conventional problems. These optimization problems have varying levels of performance, input requirements, number of iterations from the start to obtaining results and the quality of results provided. A typical optimization problem in abrasive waterjet cutting operations is choosing an adequate optimization scheme under the prevailing industrial conditions to provide quick and robust solutions to enhance operational performance



and ensure the sustainability of operations on the factory floor. The prevailing industrial conditions include a tendency towards lean practices to sustain machining operations. Here, costs are controlled and the safety and health of the operators are also guaranteed. Issues such as machining costs, machining center resources, limited budgets and more bring about the difficulty in obtaining optimal results on time and within budgets.

Consequently, in the choice of optimization method to adopt, machining managers must consider speed, agility, resilience and remarkable adaptability. An optimization method, which demonstrates the potential for all these aforementioned attributes must be used to eliminate unnecessary costs and ensure the timely delivery of the machined parts to customers. Using a non-conventional method will confine the critical highlights of a real-world optimization scheme. Nonetheless, the continually changing landscape in optimization coupled with the stricter government policies on machining operations has an inbuilt recognition of waste avoidance to ensure continuous system sustenance. This therefore makes the optimization of cutting parameters a more careful step to adopt in a complex context. Therefore, the Aquila algorithm would be a competent nature-inclined population-oriented metaheuristic optimization scheme to aid machining cutting decisions on the parametric optimization problem.

## 2.2 Aquila algorithm

The research methodology implemented in this study is shown in Figure 1. However, an extensive discussion of the Aquila algorithm that features in Figure 1 is made in this section. The Aquila optimization algorithm, developed by Abualigah et al. (2021), is a nature-inspired population-based metaheuristic algorithm inspired by Aquila's behavior in nature. The algorithm is inspired by the different hunting techniques which the Aquila uses to catch its prey. Abualigah et al. (2021) were able to derive mathematical expressions that depict the four methods used by Aquila so that the efficiency of eagle hunting can be translated into the optimization of industrial processes. There are four hunting methods used by the Aquila and all the methods are deployed depending on the situation of the prey (i.e., the proximity to the prey, the size of the prey and the speed of the prey, amongst others).

This work attempts to improve on the experimental research results conducted by Perumal et al. (2020) which sought to optimize the parameters of the abrasive waterjet machining process of Ti-6Al-2Sn-4Zr-2Mo alpha-beta alloy. The present approach is the use of a novel algorithm termed the Aquila algorithm, which mimics the eagle bird. Aquila is a particular species of eagle bird with outstanding features of exploration and exploitation of prey in a quick period. In a previous attempt using this particular experimental data by Perumal et al. (2020), Nwankiti and Oke (2022) utilized the EDAS and DFA methods to select the best parameters of the machining process. Nonetheless, it is strongly believed that a new optimization method, the Aquila algorithm should be contributed in an applied form, to the experimental data by Perumal et al. (2020). Thus, in this work, the researchers attempt to implement the Aquila algorithm to arrive at optimal cutting conditions for the Ti-6Al-2Sn-4Zr-2Mo alpha-beta alloy using the abrasive waterjet machining process. However, previously, the present authors have implemented the Perumal et al. (2020) data using the EDAS and DFA methods. Thus,

implementing the Aquila algorithm on the specified data can be useful to (1) verify the EDAS and DFA methods, and (2) arrive at another variety of optimization methods for solving this problem.

The algorithm has stages that mimic the different stages of the eagle's hunting behavior in an implementation of the mathematical model, particularly using the C++ programming code for fast procedural implementation of the hunting stages. This is for the cutting process parametric determination of the Ti-6Al-2Sn-4Zr-2Mo alpha-beta alloy. The behavior of the eagle is such that the actions taken by the eagle in the air when it is far from the prey are different from the actions embarked upon when the eagle has spotted the particular prey it desires. The actions are also different when the eagle is already approaching the prey. It is also distinct in actions when the eagle is on the ground and walking to grab the prey. So, for these four stages mentioned, the Aquila optimization tries to mimic the hunting behavior of the eagle by applying it such that at the beginning of the optimization method, it reveals the way the eagle is far from the prey is the way researchers are far from the optimal solution. However, as researchers continue to conduct the optimization, the optimal solution gets close. In some cases, one can obtain the optimal solutions. These ideas are shown in the four methods that Aquila uses in handling the hunting process. Concerning the adaptation of the various methods to the kind of prey that Aquila desires, there is a difficulty faced by the authors in understanding this. While researching, two different perspectives of the literature exist on Aquila optimization. One of the sources gives the notion that the Aquila chooses the method to embark on hunting based on the nature of the prey, including the size of the prey as well as the speed at which the prey moves when caught by the Aquila. However, on studying the paper by Abualigah et al. (2021), the impression obtained was that Aquila might not necessarily conduct the four methods in hunting a particular prey. Notwithstanding, the Aquila will always start its hunting from the expanded exploration method. The Aquila might conduct the narrowed exploration method. However, Aquila has to conduct the expanded exploitation method. Although the Aquila might not conduct all the stages of hunting (i.e., all four methods) in the optimization, Aquila has a sequence of techniques, which it must follow to capture the prey. Moreover, the various methods that Aquila uses are described here. The first method is called the expanded exploration. The aquila adapts this method when it hunts during flight and it is when it selects a desired hunting area. Moreover, exploration can be applicable when the Aquila is in the air and looks at the places to hunt with a limited view and where limited prey are available. It makes up its mind that it will land in that area. At this point, the Aquila may not know what particular prey it is to hunt, i.e., a monkey, but it has identified that this is the location it desires to land to hunt the prey. It may act on previous experience that it knows about the habitat of its prey. Aquila lands in this area also based on the boundary that it can observe at that particular time. At this time, the Aquila decides to land in the area when it feels that animals are in that area (i.e., circumference or radius). Thus, the Aquila limits its exploration to that particular radius. This might be likened to when a matrix is to be initialized in a programming attempt, to possible optimal solutions. Here, the solutions are usually within the bounds of the upper and lower



boundary conditions for the parameters that are being optimized. The second method used by the Aquila is narrowed exploration. According to Abualigah et al. (2021), narrowed exploration is used by Aquila when the prey in question is spotted from a high place. Here, the aquila begins by searching the prey after which it prepares to land and attack. Thus, circling the prey refers to the initial method of optimization. Moreover, in some cases, the optimal solution might be arrived at immediately, although this is hardly the case. The reason is that there is still a gradual testing of the mathematical solution to see if there can be a more optimal output. This could be a lower or higher value, which depends on the choice of optimization method. Notwithstanding, this is the initial stage. Moreover, the Aquila algorithm has a condition that if the number of iterations in the C++ program being implemented for the Aquila program is less than or equal to two thirds of the maximum iteration, then either the expanded exploration or the narrowed exploration is applied. However, if it is greater than this value, the

programmer (researcher) is at the later stage of the optimization. Therefore, the researcher will not apply the narrowed exploration or the expanded exploration. It implies that the researcher will apply more advanced hunting techniques. Notwithstanding, it may be said that the Aquila algorithm may adopt the expanded exploration first and then the narrowed exploration to finalize the hunting process. The third method that Aquila uses in its hunting is called expanded exploitation. Here, the aquila implements a low flight mode with slow descents in its attacks when the location of the prey has been carefully specified and the Aquila is set to land and attack the prey. This stresses that the Aquila is arriving at the optimal solution at least within that particular hunting task. So, the analogy with optimizing is that the number of iterations is gradually coming to a close or at least within the number of iterations that the researcher is implementing. Here, the researcher arrives at the optimal solution. Therefore, there is time to exploit the available possible solutions to observe which one can be the optimal option.

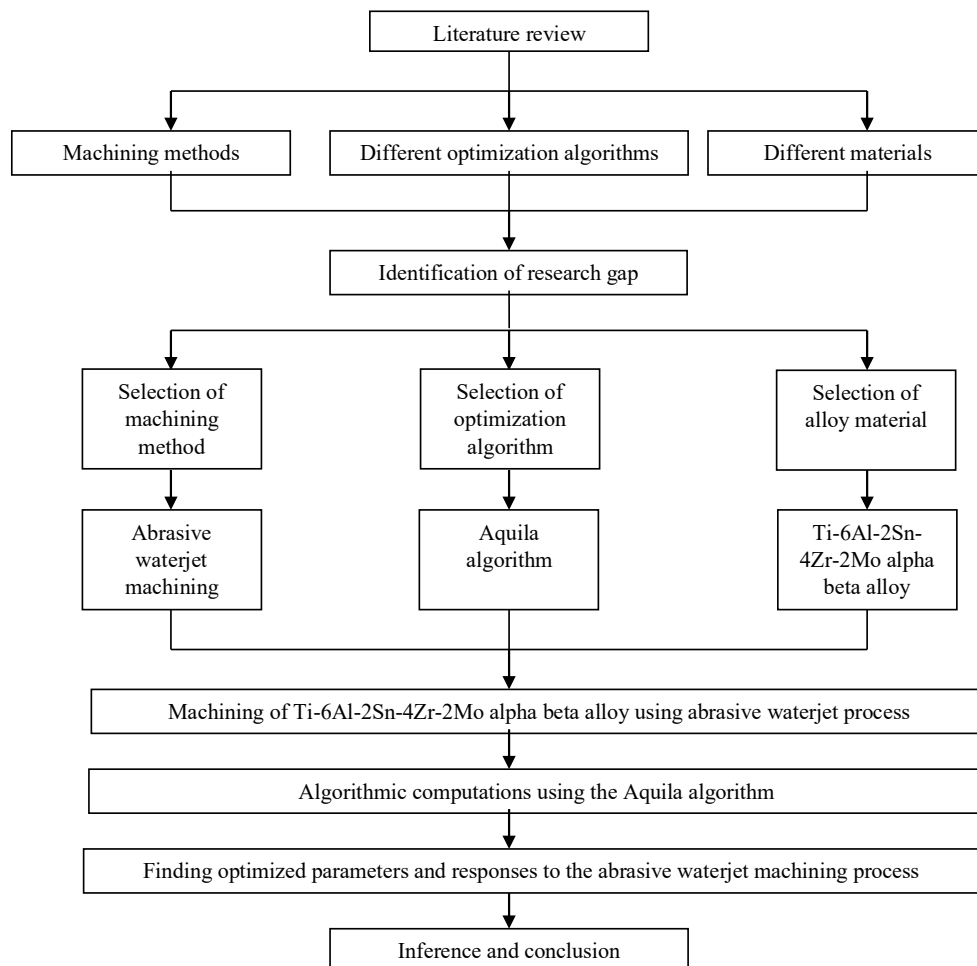


**Figure 1.** Research methodology

The fourth method that the Aquila uses to hunt the prey is narrowed exploitation. This is the method of hunting that the Aquila uses when it is close to the prey; the Aquila catches the prey by walking and grabbing it. However, whether Aquila adopts this method or not depends on randomness. For this method, a random number between three and four numbers is generated. However, if this random number is

greater than 0.5, the narrowed exploitation is taken, otherwise, the expanded exploitation is adopted. It is interesting to note that all the four methods described are represented by mathematical equations. These mathematical equations were programmed in this work to conduct the Aquila algorithmic implementation. The program was written in C++. The four methods are described as follows:

### 2.2.1 Method 1: Expanded exploration

The most common description of this method is “high soar with a vertical stoop”. The eagle rises or flies high in the air and then bend its head or body both forward and downwards. For this approach, the target, which may be a rabbit, is hunted during the flight of the Aquila. The Aquila is above the area while attempting to detect prey. Soon after, the Aquila detects the prey and makes further efforts with a low-angle glide using speed. The gliding of the eagle is a smooth effortless movement but with speed to catch the hunted prey. The next process is that the Aquila unfolds its wings and starts to catch the prey. The mathematical model for the expanded exploration behavior is shown in Equation 1.

$$X_1(t+1) = X_{best}(t) \times \left(1 - \frac{t}{T}\right) + X_m(t) - X_{best}(t) \times rand \quad (1)$$

where  $X_1(t)$  is the value of each agent at iteration  $t$ ,  $t$  is the current iteration,  $T$  is the maximum iteration.

In real life, the location of the Aquila is different from that the prey. However, in the Aquila algorithm discussed here, this is accounted for initializing the population. In Equation 1, the best solution is the target (i.e., the prey hunted) and this is shown as the first term on the right-hand side of Equation 1. The term  $X_1(t+1)$ , is the new solution in the prey hunting task performed by the Aquila algorithm. The second term,  $\left(1 - \frac{t}{T}\right)$ , is called the control exploration parameter which helps the Aquila to direct its behavior during the period that the Aquila discovers the prey in an exploration mode.  $X_m(t)$ , is the local mean value. This is the mean value for all agents that are present in the population, represented as Equation 2.

$$X_m(t) = \frac{1}{N} \sum_{i=1}^N X_i(t), \quad \forall j = 1, 2, \dots, Dim \quad (2)$$

where  $N$  is the number of agents that are present in the population,  $X_i(t)$  is the value of each agent at iteration  $t$ ,  $T$  is the maximum iteration, and  $Dim$  is the variable size.

Population size features in the formula of the mean, i.e.,  $X_m$ . The role that the population size plays here is similar to what is obtained in other optimization methods. However, the user is expected to choose the population size suitable for the problem being solved. In the present study, a population size of 6 was chosen for the present optimization problem. Moreover, the significance of the word local means at that particular instance. The word local is used because it is obtained when optimizing a factor. Consider a matrix consisting of a population of 6, which has to be optimized. Imagine also when one is optimizing the first solution and one is required to obtain the mean at that instance. This is what makes it local in a way. Notice also that the best solution is chosen at every iteration but the local is chosen when one is optimizing each of the solutions. The next term after  $X_m(t)$  is the  $X_{best}(t)$ , which is the best solution. Then we have the term “rand” which is the random value generated. Thus, in Equation (1),  $X_{best}(t)$  is considered the target of the Aquila, which is the prey. The computation (updating) will be made using positions around the best solution.

### 2.2.2 Method 2: Narrowed exploration

This is the second method which is often described as “contour of light with short glide attack”. Here, the eagle flies in a curve with a constant value such that the curve

joins points of equal value with a short but quiet continuous motion towards the prey. For this method, the prey area is first acknowledged and the Aquila then explores and forms circles above the target. It then attacks the target. This is the most common approach used by Aquila to hunt a variety of prey including sea birds. In real life, the eagle is observed moving in a circle for a long time. During this circular motion, the eagle checks whether the prey is in a steady state, running or flying. Equation 3 is the mathematical model used for this scenario.

$$X_2(t+1) = X_{best}(t) \times Levy(D) + X_R(t) + (y - x) \times rand \quad (3)$$

The left-hand side of Equation (3) is the new solution. Moving to the right-hand side of Equation (3), the first term,  $X_{best}(t)$ , is the best solution. The second term to the right-hand side of Equation (3) is levy ( $D$ ), which is the levy flight distribution that depends on Equations 4 and 5:

$$Levy(D) = \frac{s \times u \times \sigma}{|v|^{\frac{1}{\beta}}} \quad (4)$$

$$\sigma = \left( \frac{\Gamma(1+\beta) \times \sin\left(\frac{\pi\beta}{2}\right)}{\Gamma\left(\frac{1+\beta}{2}\right) \times \beta \times 2^{\left(\frac{\beta-1}{2}\right)}} \right) \quad (5)$$

where  $r_1$  = Fixed between 1 and 20,  $s = 0.01$ ,  $\beta = 1.5$ , and  $\omega = 0.005$ .

The spiral moves of the Aquila, which is calculated by the function  $X_R(t)$  that is obtained in the generation of a random solution in the range 1 to  $N$ . The random number is generated by the term  $(y - x)$  [rand]. Equations 6 to 10 support this idea.

$$y = r \times \cos(\theta) \quad (6)$$

$$x = r \times \sin(\theta) \quad (7)$$

$$r = r_1 + u \times D_1 \quad (8)$$

$$\theta = -\omega \times D_1 \times \theta_1 \quad (9)$$

$$\theta_1 = \frac{3 \times \pi}{2} \quad (10)$$

where  $y$ ,  $r$ ,  $\theta$ ,  $x$ ,  $u$ ,  $r_1$ ,  $D_1$ ,  $\omega$ ,  $\theta_1$ , and  $\pi$  are the hunting coefficients and terms.

### 2.2.3 Method 3: Expanded exploitation

Here, the Aquila has a “low flight with a slow descent attack”. The Aquila selects the area and recognizes the target (potential prey). It then explores the area and takes a slow landing before attacking the prey. The mathematical model for the behavior is shown in Equation 11:

$$X_3(t+1) = X_{best}(t) - X_m(t) \times \alpha - rand + (((UB - LB) \times rand + LB) \times rand + LB) \times \delta \quad (11)$$

On the left-hand side of Equation 11 is the new solution represented as  $X_3(t+1)$ . On the right-hand side of Equation 11 is the first term,  $X_{best}(t)$ , which is the best solution and the main target. The second term on the right-hand side is  $X_m(t)$ , the location mean value, calculated by finding the average of all agents. The next term is an exploitation parameter. Next,  $UB$  is the upper boundary while  $LB$  is the lower boundary. The term “rand” is for the generated

random number, which is normally distributed between 0 and 1. The last term,  $\delta$ , is an exploitation parameter.

#### 2.2.4 Method 4: Narrowed exploitation

This is described as a “walk-and-goal strategy” for prey hunting in the Aquila algorithm implementation. Here, the Aquila walks on the land, gets closer to the prey and then attacks. The mathematical model for method 4 is shown in Equation 12, with the details of quality function (QF) explained in Equation 13. The method is often used to attack large-sized prey such as the baboon. Furthermore, the Aquila attempts to pull its target in two instances of  $G_1$  and  $G_2$ , which represent motion and flight modes, respectively (Equations 14 and 15). It has a simplified model whose details are considered in the C++ programming code of this work.

$$X_4(t+1) = QF \times X_{best}(t) - (G_1 \times X(t) \times rand) - (G_2 \times Levy(D) + rand \times G_1) \quad (12)$$

where  $X_4(t+1)$  is the solution of the next iteration of  $t$ .

QF is the quality function used to provide equilibrium to search strategies.

$$QF(t) = t^{\frac{2 \times rand - 1}{(1-T)^2}} \quad (13)$$

$$G_1 = 2 \times rand - 1 \quad (14)$$

$$G_2 = 2 \times \left(1 - \frac{t}{T}\right) \quad (15)$$

where rand represents random numbers between 0 and 1,  $t$  is the current iteration, and  $T$  is the maximum iteration.

### 3. RESULTS AND DISCUSSION

The steps to apply the Aquila algorithm in a general sense have been stated in the methodology. However, to validate the claim that the Aquila algorithm works in a practical sense, data collected from Perumal et al. (2020) in an abrasive waterjet process context, particularly in the machining of Ti-6Al-2Sn-4Zr-2Mo alpha-beta alloy, was extracted and used to test the Aquila algorithm. Notice that a computer program was developed and run for the implementation of the Aquila algorithm using the C++ program and the results obtained are discussed in this section. Moreover, among the requirements for the implementation of the Aquila algorithm for the abrasive waterjet process are two main issues. The first is the development of the boundaries for all the parameters used in the work and the second issue is the formulation of the regression model for the outputs (MRR and SR), which are to be substituted into the objective function module of the Aquila algorithm. This objective function is to be either minimized or maximized according to the implication of optimizing these outputs. While the second aspect, vis-à-vis the development of the empirical mathematical model in regression form, is treated as a separate sub-section; the development of boundary conditions for the parameters is tackled here. To start with, the experimental design data L27 orthogonal array of Perumal et al. (2020) (Table 1) is referenced here for analysis.

The boundaries of interest are the lower and upper limits of each of the variables (parameters), which can be interpreted from the range of values for each parameter. By observing the values under the second column, which shows the abrasive waterjet pressure, a minimum of 220 bar was observed for experimental trials 1 to 9 and hence 220 bar becomes the lower boundary of the values for the pressure. Also, the highest value of the pressure under, the abrasive waterjet pressure parameters is 260 bar, which occurs at experimental trials 20 to 27. Accordingly, 260 bar is taken as the upper boundary of the abrasive waterjet pressure. Similarly, for the traverse speed, the lowest and highest values are 20 mm/min and 40 mm/min, respectively. These are the lower and upper boundaries for the abrasive waterjet pressure.

Furthermore, for the stand-off distance, the lowest and highest values are 1 mm and 3 mm, which are the lower and upper boundaries, respectively.

#### 3.1 Formulating objective functions

A single objective function is formed with a focus on the objective function for the material removal rate at one time while at the other time, the focus shifts to the surface roughness response. Thus, the Aquila algorithm takes on this single objective as inputs and produces output, which are the desired parametric values. However, this stage is the pre-implementation procedure of the Aquila algorithm. Thus, the formulation of the objective function in this segment was achieved using linear regression. This was achieved by deriving the expression for the regression model. The idea of derivation is to best fit the abrasive waterjet cutting data. This data consists of the material removal rate (MRR) as a response, while the parameters concerned are the waterjet pressure (WJP), traverse speed (TS) and stand-off-distance (SOD). This is on one side of the analysis. On the other side of the analysis, the surface roughness (Ra) represents the response while the parameters remain the WJP, TS, and SOD. Consider the X and Y axis as planes of reference. Now, the data points to use are those formed from the orthogonal array implementation that produced 27 sets of data for each of the parameters and responses for the abrasive waterjet process (Table 1). From Table 1, 27 data points are given, which may be represented by (MRR<sub>1</sub>, WJP<sub>1</sub>), (MRR<sub>2</sub>, WJP<sub>2</sub>), (MRR<sub>3</sub>, WJP<sub>3</sub>), and (MRR<sub>27</sub>, WJP<sub>27</sub>). This was for a set of relationships. For the other set of relationships between MRR and TS, the WJP<sub>1</sub> WJP<sub>2</sub>, WJP<sub>3</sub>, WJP<sub>27</sub>, were replaced with TS<sub>1</sub>, TS<sub>2</sub>, TS<sub>3</sub>, TS<sub>27</sub>, respectively, as (MRR<sub>1</sub>, TS<sub>1</sub>), (MRR<sub>2</sub>, TS<sub>2</sub>), (MRR<sub>3</sub>, TS<sub>3</sub>), and (MRR<sub>27</sub>, TS<sub>27</sub>). Likewise, MRR has relationships with the various data points of SOD as represented by (MRR<sub>1</sub>, SOD<sub>1</sub>), (MRR<sub>2</sub>, SOD<sub>2</sub>), and (MRR<sub>27</sub>, SOD<sub>27</sub>). These relationships of MRR have been seen to involve WJP, TS, and SOD, all of which range from 1 to 27 data points. Thus, for all the data points involving MRR<sub>1-27</sub> in relationship with WJP<sub>1-27</sub>, TS<sub>1-27</sub>, and SOD<sub>1-27</sub>, the idea was to “best” fit a curve to it. That curve may be Equation 16:

$$MRR = a_0 WJP + a_1 TS + a_3 SOD + a_4 (WJP)^2 + a_5 TS^2 + a_6 SOD^2 + a_7 (WJP)(TS) + a_8 (WJP)(SOD) + a_9 (TS)(SOD) \quad (16)$$

where  $a_0, a_1, a_2, a_3, a_4, a_5, a_6, a_7, a_8$ , and  $a_9$  are constants.

**Table 1.** Experimental results for the abrasive waterjet process

Trial no	WJP (bar)	TS (mm/min)	SOD (mm)	MRR (mm <sup>3</sup> /min)	Ra (μm)
1	220	20	1	81.3333	3.0006
2	220	20	2	84.1666	2.8713
3	220	20	3	86.8333	2.6366
4	220	30	1	116.5000	2.8620
5	220	30	2	119.2500	3.0583
6	220	30	3	121.2500	2.8153
7	220	40	1	151.6670	2.7560
8	220	40	2	153.3330	3.7006
9	220	40	3	160.2130	3.2143
10	240	20	1	78.3330	2.7311
11	240	20	2	82.5140	2.7893
12	240	20	3	85.5010	2.8156
13	240	30	1	116.1100	2.8030
14	240	30	2	121.2500	3.0353
15	240	30	3	125.2500	2.9540
16	240	40	1	150.2400	3.0516
17	240	40	2	159.0120	2.9406
18	240	40	3	163.3330	3.2403
19	260	20	1	80.1230	2.4000
20	260	20	2	84.4500	2.6930
21	260	20	3	87.3333	3.0670
22	260	30	1	115.7500	2.4681
23	260	30	2	119.500	2.9566
24	260	30	3	125.1200	3.3196
25	260	40	1	150.6670	3.0363
26	260	40	2	157.2040	3.1643
27	260	40	3	165.3330	3.5261

(Source: Perumal et al., 2020)

Likewise, for the second response, Ra relationship can be established between Ra and all other variables and constants as in Equation 16. However, the values of the constants  $a_0$  to  $a_9$  will be different in this case. Now consider Equation 16, which suggests that, given the 27 data points, a curve representation of the data points is desired. Eventually, the aim is to minimize the amount of differences which occur between the observed values of WJP<sub>1</sub>, TS, and SOD, as well as what the curve will predict. There are differences in 27 instances since 27 data points are considered. The predicted value at one of the 27 instances may be represented by an equation such that if the values of WJP, TS, and SOD at an instance are used, one will obtain almost the values on the curve. By observing the amount of residuals, the predicted value subtracted from the observed values gives the residual at each point. It is desired to make the residual as little as possible and one of the criteria used is the sum of the squares of the residuals. This is obtained by squaring the error at each point and adding them together. The criterion is referred to as the least square error of the regression model. Notice that in achieving the least square errors, the only control in the hand of the researcher is the constants of the equations.

Furthermore, the derivative of the problem involves obtaining the derivative of the sum of the squares of the residuals with respect to each of the constants  $a_0$  to  $a_9$ . Here nine equations and nine unknowns may be developed, which can be solved mathematically. This will help to find out what  $a_0$  to  $a_9$  are. The proof of this analysis will not be done as it may become cumbersome and the Minitab 18 (2020) software is used to solve the problem to obtain the equations relating MRR to WJP, TS, and SOD as well as Ra in relation to WJP, TS, and SOD.

After developing the empirical models for both MRR and  $R_a$ , it was necessary to obtain some statistical measures for each of the outputs regarding the regression model formed. Thus, for MRR, it was found that the S, R-sq, R-sq(adj) and R-sq(pred) are 1.3054, 99.99%, 99.99%, and 99.98%. A key measure is the R-sq, which gives 99.99%, indicating that when Equation 17 is used to predict the MRR, only 0.01% error is possible at a 95% confidence level.

Compared with SR which gives S, R-sq, R-sq(adj), and R-sq(pred) as 0.1939, 99.72%, 99.57%, and 99.26% respectively, MRR exceeds SR in the predictive performance of its ability to retrace experimental data's path. This



means that R-sq, which gives 99.72% shows 0.28% error at 95% confidence level when used to predict the experimental data (Equation 18). It shows that 0.28% for SR is worse than 0.01% for MRR. In summary, the prediction equations for MRR and SR are given as Equations 17 and 18:

$$\text{MRR} = 0.2577\text{WJP} + 2.535\text{TS} - 11.82\text{SOD} - 0.000898\text{WJP} * \text{WJP} + 0.00080\text{TS} * \text{TS} - 0.030\text{SOD} * \text{SOD} + 0.00339\text{WJP} * \text{TS} + 0.0511\text{WJP} * \text{SOD} + 0.1365\text{TS} * \text{SOD} \quad (17)$$

$$\text{Ra} = 0.0411\text{WJP} - 0.0508\text{TS} - 1.516\text{SOD} - 0.000126\text{WJP} * \text{WJP} + 0.000550\text{TS} * \text{TS} - 0.0979\text{SOD} * \text{SOD} + 0.000108\text{WJP} * \text{TS} + 0.00777\text{WJP} * \text{SOD} + 0.00604 \text{TS} * \text{SOD} \quad (18)$$

This is now at a stage where all the calculated inputs and outputs will be substituted into the Aquila algorithm. However, some additional information is needed for the code implementation: The population size has to be determined, which is given as 6. This further means that six Aquila, chosen based on the experience of the present authors, will be used. Furthermore, the number of iterations is chosen as 300, which is also based on the programming experience of the authors. So, the next step is to randomly initialize the population, which is achieved by using Equation 19:

$$x = L + r(U - L) \quad (19)$$

where  $L$  is the lower boundary,  $r$  is the random number generated between 0 and 1,  $U$  is the upper boundary.

On substituting the various values of the upper and lower boundaries, and generating a new random number in each instance, the data in Table 2 is obtained.

**Table 2.** Data for six Aquila

Aquila/ location	WJP	TS	SOD	MRR
1	253.309	20.0824	2.65581	86.1878
2	250.162	20.968	2.30314	88.208
3	250.783	39.4891	1.31831	151.44
4	231.153	23.6628	1.6523	95.8037
5	255.649	20.5567	1.36091	82.9109
6	234.438	28.5501	1.66976	113.466

In Table 2, only the columns for WJP, TS, and SOD can be obtained using the boundary data as well as generated random numbers. However, by substituting these values in Equation 16, the values of MRR, which occupies the last column are computed. This is the output value or fitness value in this algorithmic operation. Then, the first iteration is performed, which are the steps taken in the application of the Aquila algorithm on the first element. This entails the selection of the best item among all the prospective locations based on the fitness value. Moreover, the best possible location from the population is dependent on the output value (i.e., the material removal rate in this case) and the choice of optimization either minimization or maximization. In this case, the researchers desire the greatest material removal rate possible, hence maximization. It is then consequential that the best among the population of the prospective location will be the one with the largest fitness value. Regarding Table 2, the best solution is the

prospective location of Aquila 3 at position 3, which gives WJP, TS, SOD, and MRR of 250.783 bar, 39.4891 mm/min, 1.31831 mm, and 151.44 mm<sup>3</sup>/min, respectively.

To this end, for each of the prospective locations, some tasks were conducted. Take note that, for the first prospective location, WJP, TS, SOD, and MRR are 253.309 bar, 20.0824 mm/min, 2.65581 mm, and 86.1878 mm<sup>3</sup>/min, respectively. However, the mean of the current solution,  $X_m$ , needs to be updated using Equation 2.  $X_m$  is the mean of all the elements or prospective solutions at that particular instance. This gives a new set of values for WJP, TS, SOD, and MRR as 245.916 bar, 25.5515 mm/min, 1.82671 mm, and 103.003 mm<sup>3</sup>/min, respectively. Take note also that WJP is found, for example, by finding the sum of WJP from the first to the sixth prospective locations, which is then divided by  $N$  (i.e., 6 in this case). The other values are calculated in that manner. However, it is in turn to choose the method to be used to explore the current prospective location. Then the condition of  $t \leq 2/3T$  also has to be satisfied as we are currently in the first iteration of the 300 iterations planned for the program. Next, the researcher chooses a random number between 0 and 1. Here, the number chosen should be specified, which is 0.833125, compared with 0.5. The value 0.833125 is greater than 0.5 and method 2, which is the narrowed exploration, is utilized to explore the current prospective location. Furthermore, to conduct the narrowed exploration procedure, Equation 3 is used. Here, the  $X_{best}(t)$  is given as [250.783, 39.4891, 1.31831, 151.44], which is a component of the calculation. A second component of the computation is the levy ( $D$ ), which is obtained as 0.012504 when the values of 0.833125, 0.6966, 0.316202, and 1.5 are for the respective parameters of  $U$ ,  $\sigma$  and  $\beta$  while  $s$  is 0.1, a fixed value. Take note that  $u$  being 0.833125 was randomly chosen. However,  $V$ ; which is 0.316202 is also randomly chosen. Thus, because,  $X_R(t)$  is a random solution in the range of  $[1N]$ , the 6th prospective solution is chosen as the random solution, which is stated as:

$$X_R(t) = [234.438, 28.5501, 1.66976, 113.466]$$

Now, by substituting in Equations (4) to (10) and given that  $D_1 = [1 \ 2 \ 3 \ 4]$ ,  $r_1 = 15$  (i.e., a fixed value between 1 and 20), then  $r$  is given as [15.0056, 15.0113, 15.0169]. Also given that  $Q_1 = 4.71239$ ,  $\omega = 0.005$  (i.e., fixed),  $Q$  is calculated as [4.70739, 4.70239, 4.69739]. Furthermore, take note that  $y = [0.0750279 - 0.15011 - 0.0225246]$  while  $x = [-15.0055 - 15.0105 - 15.0153]$  is generated. Also, note that  $r_1$  takes a value between 1 and 20 fixed for the number of searches.  $U$  is fixed at 0.00565,  $D_1$  is an integer number from 1 to the length of the search space (Dim), where  $\omega$  is fixed at 0.005. All these values are introduced into Equation 3 for the new solution of  $X_2(t + 1)$  as

$$X_2(t + 1) = [237.702 \ 39.3192 \ 6.23424]$$

Here, a boundary check is conducted on the respective value of  $X_2$  to ensure that they fall within the bounds set for the elements initially. Any value that falls below the lower boundary is replaced with the lower boundary and any value that falls above the upper boundary is replaced with the upper boundary. This step is important to ensure the accuracy of results and that the solution progresses within the bounds. Now, after the boundary check,

$$X_2(t+1) = [237.702 \ 39.3192 \ 3]$$

It is observed that the value of the standoff distance has been replaced with its upper boundary, while other values remain the same because they fall within the bounds. Furthermore, after the  $X_2(t+1)$  has been inserted into the objective functions, a performance yield of 159.922 was noticed as the force. Therefore,  $X_2(t+1) = [237.702 \ 39.3192 \ 3.15922]$ .

Next is to conduct greedy selection. The  $F(t)$  of the new solution is given as 159.92 while the  $F(t)$  of the current solution is 86.1878. However, the objective function is to maximize the material removal rate, which yields a larger value of the material removal rate than the former solution. Therefore, a replacement will take place. The same steps are repeated from step 3 to step 6 for all the prospective locations in the current iteration. For the subsequent iterations, the steps from step 2 are repeated all over again. At the end of every iteration, the locations with the best performance are obtained. Furthermore, after 300 iterations the best solutions are displaced as follows:

Iteration 1: 250.783, 39.4891, 1.31831, 151.44  
 Iteration 2: 237.702, 39.3192, 3, 159.922  
 Iteration 3: 260, 40, 3, 164.741  
 Iteration 4: 260, 40, 3, 164.741  
 Iteration 298: 260, 40, 3, 164.741  
 Iteration 299: 260, 40, 3, 164.741  
 Iteration 300: 260, 40, 3, 164.741

Now, observing the convergence at iteration 300, the values obtained are taken as the best solutions. The optimal solution obtained after 300 iterations were WJP, TS, SOD, and MRR at 260 bar, 40 mm/min, 3 mm, and 164.74 mm<sup>3</sup>/min, respectively. This is the solution considering the MRR. However, surface roughness was also optimized using the Aquila algorithm and the results obtained after 300 iterations were WJP, TS, SOD, and SR at 256.272 bar, 24.0162 mm/min, 1.00214 mm, and 2.5429 mm<sup>3</sup>/min, respectively.

### 3.2 Correlation analysis

The empirical equation generated by the material removal rate was used in the determination of optimal parameters for the Ti-6Al-2Sn-4Zr-2Mo alpha-beta alloy which yielded some optimal values of WJP, TS, and SOD. When a surface roughness empirical equation was used to obtain optimal values for the same parameters, correlation analysis was done with and without the incorporation of the responses into the analysis. A correlation value of 0.99865 was achieved, indicating 99.87% with an error of 0.13% obtained at a 95% confidence level without the responses included in the analysis. This high correlation indicates that the two methods of MRR and SR are reliable in predicting the optimal values. For the situation where the MRR and SR were included in the analysis, the correlation value dropped to 0.794519 i.e., 79.45% and an error of 20.55% at a 95% degree of confidence. Although the value is strongly positive, it is weaker than the earlier obtained value without the responses considered in the correlation analysis.

### 3.3 Contributions to knowledge

This article provides some contributions to the machining literature. First, the literature on abrasive waterjet cutting

operations has been advanced by introducing a novel method called the Aquila algorithm to optimize the cutting process parameters in a four-phase methodology of exploration and exploitation: expanded exploration, narrowed exploration, expanded exploitation and narrowed exploitation. Since 2021, when Abualigah et al. (2021) contributed this unique method of optimization, the present article is one of the most recent attempts at expanding the scope of the application of the Aquila algorithm. Machining is one rare application of the Aquila algorithm, so this is the first application of the Aquila algorithm in abrasive waterjet cutting operations. The results chronicle the significance of machining predictions in providing standards with which operations can be compared to achieve machining goals. For example, it is known that the workforce should aim to achieve the optimal results obtained after 300 iterations for both the material removal rate and the surface roughness. For material removal rate, the optimal results are 260 bar of WJP, 40 mm/min of TS, and 3 mm of SOD, while the MRR is 164.74 mm<sup>3</sup>/min. However, for the surface roughness, the optimal solution is 256.27 bar of WJP, 24.02 mm/min of TS, and 1 mm to SOD, while the Ra is 2.54 mm.

## 4. CONCLUSION

The abrasive waterjet process parameters for the Ti-6Al-2Sn-4Zr-2Mo alpha-beta alloy were investigated and analyzed. In this study, the optimization characteristics of the process and parameters were studied on the outcomes of the process using the Aquila algorithm. The parameters studied are the traverse speed, abrasive waterjet pressure and stand-off distance, while the responses are the material removal rate and surface roughness. Empirical modelling and optimization were conducted using the multiple regression model and the model was substituted into the Aquila algorithm after being extracted from the Minitab 18 (2020) software and classification tool. The following conclusions are drawn from this investigation:

1. The optimal parameters at the convergence of the results after 300 iterations are WJP, TS, SOD, and MRR of 260 bar, 40 mm/min, 3 mm, and 164.74 mm<sup>3</sup>/min, respectively. This is when the response considers the material removal rate. Considering the surface roughness as the output, the optimal solution is WJP, TS, SOD, and SR of 256.27 bar, 24.54 mm<sup>3</sup>/min, 1.00 mm, and 2.54 mm<sup>3</sup>/min, respectively.
2. A correlation of 99.87% was obtained when the parameters obtained by the MRR and SR empirical equation were compared. This shows an error of 0.13%. The result is acceptable.
3. The indicated optimal values of the parameters under the surface roughness outcome and the material removal rate results were attained to ascertain minimum surface roughness and maximum material removal rate.
4. The Aquila algorithm obtained two predictive methods for material removal rate and surface roughness, which accurately predict the optimal thresholds of the important parameters of the system, including traverse speed, stand-off distance, and abrasive waterjet pressure.
5. The Aquila algorithm is very efficient and competently evaluates the material removal rate and surface roughness of the abrasive waterjet machining process while using the Ti-6Al-2Sn-4Zr-2Mo alpha-beta

alloy. Moreover, the study may be a reference point for other alloys (i.e., super alloys) and effective machining can be obtained easily. Furthermore, it is feasible to use the Aquila algorithm to establish the optimal conditions of abrasive waterjet machining for Ti-6Al-2Sn-4Zr-2Mo alpha-beta alloy.

6. It is the first time the Aquila algorithm was used to optimize decisions for the abrasive waterjet machining process. The use of Ti-6Al-2Sn-4Zr-2Mo alpha-beta alloy was effective in this respect.

7. The validation of the Aquila algorithm was achieved using the data on the Ti-6Al-2Sn-4Zr-2Mo alpha-beta alloy.

8. In the present study, data were fed manually into the computer system for decision-making. Yet, it is not possible to automate the data collection system. The inability to automate the data collection system is at present a limitation. To overcome this limitation, connections should be made with the internet such that data will be stored in a cloud, which may be retrieved at will for analysis.

9. In utilizing the Aquila algorithm to make optimization decisions, boundaries should be stated such that the maximum values in an orthogonal array represent a criterion maximized such as the material removal rate and minimum values indicated for a criterion being minimized such as surface roughness. However, when a parameter cannot be classified into these categories such that it is nominal, understanding the optimization direction could be the subject of future investigation.

10. In this study, material removal rate and surface roughness were used as responses in the abrasive waterjet process. However, in future work, operating time and hardness could be investigated as additional responses for the system, both at a time and simultaneously. Also, only three parameters namely traverse speed, abrasive waterjet pressure and stand-off distance were considered. However, the range of parameters could be extended to include the speed of the rotating surface and nozzle tilt angle.

## REFERENCES

- Abualigah, L., Yousri, D., Abd Elaziz, M., Ewees, A. A., Alqaness M. A. A., & Gandomi, A. H. (2021). Aquila optimizer: A novel meta-heuristic optimization algorithm. *Computers and Industrial Engineering*, 157, Article 107250. <https://doi.org/10.1016/j.cie.2021.107250>
- Ay, M., Çaydaş, U., & Haşcalık, A. (2010). Effect of traverse speed on abrasive waterjet machining of age hardened Inconel 718 nickel-based superalloy. *Materials and Manufacturing Processes*, 25(10), 1160–1165. <https://doi.org/10.1080/10426914.2010.502953>
- Boud, F., Murray, J. W., Loo, L. F., Clare, A. T., & Kinnell, P. K. (2014). Soluble abrasives for waterjet machining. *Materials and Manufacturing Processes*, 29(11–12), 1346–1352. <https://doi.org/10.1080/10426914.2014.930949>
- Chakraborty, S., & Mitra, A. (2018). Parametric optimization of abrasive water-jet machining processes using grey wolf optimizer. *Materials and Manufacturing Processes*, 33(13), 1471–1482. <https://doi.org/10.1080/10426914.2018.1453158>
- Fan, C., Wang, W., & Tian, J. (2024). Flexible job shop scheduling with stochastic machine breakdowns by an improved tuna swarm optimization algorithm. *Journal of Manufacturing Systems*, 74, 180–197. <https://doi.org/10.1016/j.jmsy.2024.03.002>
- Halteh, K., AlKhoury, R., Ziadat, S. A., Gepp, A., & Kumar, K. (2024). Using machine learning techniques to assess the financial impact of the COVID-19 pandemic on the global aviation industry. *Transportation Research Interdisciplinary Perspectives*, 24, Article 101043. <https://doi.org/10.1016/j.trip.2024.101043>
- Hussain, A., Janjua, T. A. M., Malik, A. N., Najib, A., & Khan, S. A. (2024). Health monitoring of CNC machining processes using machine learning and wavelet packet transform. *Mechanical Systems and Signal Processing*, 212, Article 111326. <https://doi.org/10.1016/j.ymssp.2024.111326>
- Ishfaq, K., Mufti, N. A., Ahmed, N., & Pervaiz, S. (2019). Abrasive waterjet cutting of clad material: Kerf taper and MRR analysis. *Materials and Manufacturing Processes*, 34(5), 554–553. <https://doi.org/10.1080/10426914.2018.1544710>
- Kalirasu, S., Rajini, N., Rajesh, S., Seingchin, S., & Ramaswamy, S. N. (2018). AWJ machinability performance of CS/UPR composites with the effect of chemical treatment. *Materials and Manufacturing Processes*, 33(4), 452–461. <https://doi.org/10.1080/10426914.2017>
- Kant, R., & Dharmi, S. S. (2021). Investigating process parameters of abrasive water jet machine using EN31. *Materials and Manufacturing Processes*, 36(14), 1597–1603. <https://doi.org/10.1080/10426914.2021.1914849>
- Karakurt, I., Aydin, G., & Aydiner, K. (2012). An experimental study on the depth of cut of granite in abrasive waterjet cutting. *Materials and Manufacturing Processes*, 27(5), 538–544. <https://doi.org/10.1080/10426914.2011.593231>
- Li, W., Zhu, H., Wang, J., & Huang, C. (2016). Radial-mode abrasive waterjet turning of short carbon-fibre-reinforced plastics. *Machining Science and Technology*, 20(2), 231–248. <https://doi.org/10.1080/10910344.2016.1165836>
- Mezgebe, T. T., Gebreslassie, M. G., Sibhato, H., & Bahta, S. T. (2023). Intelligent manufacturing eco-system: A post COVID-19 recovery and growth opportunity for manufacturing industry in Sub-Saharan countries. *Scientific African*, 19, Article e01547. <https://doi.org/10.1016/j.sciaf.2023.e01547>
- Nakandala, D. (2024). Impact of industry 4.0 technologies on operations resilience: Adverse effects of COVID-19 as a moderator. *Procedia Computer Science*, 232, 3258–3267. <https://doi.org/10.1016/j.procs.2024.02.141>
- Naresh Babu, M., & Muthukrishnan, N. (2015). Investigation of multiple process parameters in abrasive water jet machining of tiles. *Journal of the Chinese Institute of Engineers*, 38(6), 692–700. <https://doi.org/10.1080/02533839.2015.1010944>
- Nwankiti, U. S., & Oke, S. A. (2022). Optimal cutting conditions of abrasive waterjet cutting for Ti-6Al-2Sn-2Mo alpha-beta alloy using EDAS and DFA methods. *Gazi University Journal of Science Part A: Engineering and Innovation*, 9(3), 233–250. <https://doi.org/10.54287/gujsa.1135609>
- Pancaldi, F., Rubini, R., & Cocconcelli, M. (2023). On the performance comparison of diagnostic techniques in machine monitoring. *Mechanical Systems and Signal Processing*, 205, Article 110872. <https://doi.org/10.1016/j.ymssp.2023.110872>
- Perumal, A., Azhagurajan, A., Kumar, S. S., Kailasanathan, C., Rajan, R. P., Rajan, A. J., Venkatesan, G., & Rajkumar,



- P. R. (2020). Experimental investigation on surface morphology and parametric optimization of Ti-6Al-2Sn-4Zr-2Mo alpha-beta alloy through AWJM. *Tierärztliche Praxis*, 40, 1681–1702.
- Sadasivam, B., & Arola, D. (2012). An examination of abrasive waterjet peening with elastic pre-stress and the effects of boundary conditions. *Machining Science and Technology*, 16(1), 71–95. <https://doi.org/10.1080/10910344.2012.648565>
- Srinivas, S., & Ramesh Babu, N. (2012). Penetration ability of abrasive waterjets in cutting of aluminum-silicon carbide particulate metal matrix composites. *Machining Science and Technology*, 16(3), 337–354. <https://doi.org/10.1080/10910344.2012.698935>
- Thakur, R. K., Singh, K. K., & Ramkumar, J. (2021). Impact of nanoclay filler reinforcement on CFRP composite performance during abrasive water jet machining. *Materials and Manufacturing Processes*, 36(11), 1264–1273. <https://doi.org/10.1080/10426914.2021.1906896>
- Tripathi, D. R., Vachhani, K. H., Bandhu, D., Kumari, S., Kuma, V. R., & Abhishek, K. (2021). Experimental investigation and optimization of abrasive waterjet machining parameters for GFRP composites using metaphor-less algorithms. *Materials and Manufacturing Processes*, 36(7), 803–813. <https://doi.org/10.1080/10426914.2020.1866193>
- Wang, J., Kuriyagawa, T., & Huang, C. Z. (2003). An experimental study to enhance the cutting performance in abrasive waterjet machining. *Machining Science and Technology*, 7(2), 191–207. <https://doi.org/10.1081/MST-120022777>
- Wang, J., & Zhong, Y. (2009). Enhancing the depth of cut in abrasive waterjet cutting of alumina ceramics by using multipass cutting with nozzle oscillation. *Machining Science and Technology*, 13(1), 76–91. <https://doi.org/10.1080/10910340902776085>
- Xu, Y., Qamsane, Y., Puchala, S., Januszczyk, A., Tilbury, D. M., & Barton, K. (2024). A data-driven approach toward a machine- and system-level performance monitoring digital twin for production lines. *Computers in Industry*, 157–158, Article 104086. <https://doi.org/10.1016/j.compind.2024.104086>
- Yuvaraj, N., & Kumar, M. P. (2017). Study and evaluation of abrasive water jet cutting performance on AA5083-H32 aluminum alloy by varying the jet impingement angles with different abrasive mesh sizes. *Machining Science and Technology*, 21(3), 385–415. <https://doi.org/10.1080/10910344.2017.1283958>
- Zhang, S., & Li, X. (2010). Theoretical analysis of piercing delicate materials with abrasive water-jet. *Journal of the Chinese Institute of Engineers*, 33(7), 1015–1019. <https://doi.org/10.1080/02533839.2010.9671690>
- Zhang, Y., Du, G., Li, H., Yang, Y., Zhang, H., Xu, X., & Gong, Y. (2024). Multi-objective optimization of machining parameters based on an improved Hopfield neural network for STEP-NC manufacturing. *Journal of Manufacturing Systems*, 74, 222–232. <https://doi.org/10.1016/j.jmsy.2024.03.006>
- Zhong, Z. W., & Han, Z. Z. (2002). Turning of glass with abrasive waterjet. *Materials and Manufacturing Processes*, 17(3), 339–349. <https://doi.org/10.1081/AMP-120005380>